Lyapunov-Based Distributed Control of the Safety Factor Profile in a Tokamak Plasma

Federico Bribiesca Argomedo, Emmanuel Witrant, Christophe Prieur, Sylvain Brémond, Rémy Nouailletas, Jean-François Artaud

Lyapunov-Based Distributed Control of the Safety Factor Profile in a Tokamak Plasma

Federico Bribiesca Argomedo[1], Emmanuel Witrant[1], Christophe Prieur[1], Sylvain Brémond[2], Rémy Nouailletas[2], and Jean-François Artaud[2]

[1] Université de Grenoble / UJF / CNRS, GIPSA-lab UMR 5216, BP 46, F-38402 St. Martin D'Hères, France. Email: federico.bribiesca-argomedo@gipsa-lab.fr
[2] CEA, IRFM F-13108, Saint Paul-lez-Durance, France.

Abstract. A real-time model-based controller is developed for the tracking of the distributed safety-factor profile in a tokamak plasma. Using relevant physical models and simplifying assumptions, theoretical stability and robustness guarantees were obtained using a Lyapunov function. This approach considers the couplings between the poloidal flux diffusion equation, the time-varying temperature profiles and an independent total plasma current control. The actuator chosen for the safety factor profile tracking is the Lower Hybrid Current Drive, although the results presented can be easily extended to any non-inductive current source. The performance and robustness of the proposed control law is evaluated with a physics-oriented simulation code on Tore Supra experimental test cases.

1. Introduction

Real time control of internal profiles within a tokamak plasma is a key issue to achieve (and maintain) in a safe manner high-performance operation. Given the high uncertainty in online profile reconstruction and measurements, as well as in the modeling of transport phenomena inside the plasma, controlling these internal profiles is a very challenging task and necessitates robust feedback approaches. In particular, an adequate control of the safety factor profile or *q-profile*, which is determined by the relationship between the *toroidal* and the *poloidal* components of the magnetic field, is very important for the plasma discharge MHD stability and possible enhanced energy confinement. An overview of emerging and existing challenges of tokamak plasma control is given in [1, 2]. For a discussion on advanced tokamak scenarios, refer for instance to [3, 4] and [5].

In this article, the problem of controlling the safety factor profile (or q-profile) by controlling the gradient of the poloidal magnetic flux profile in a tokamak plasma is considered. The control design is based on the distributed control-oriented model proposed in [6], whereas it is assesed in simulation using the physics-oriented code METIS, a module of the CRONOS suite of codes, suitable for closed-loop control simulations [7]. The poloidal magnetic flux, denoted $\psi(R, Z)$, is defined as the flux per radian of the magnetic field $\boldsymbol{B}(R, Z)$ through a disc centered on the toroidal axis at height Z, having a radius R and surface $\boldsymbol{S}$, as depicted in Fig. 1. As the safety

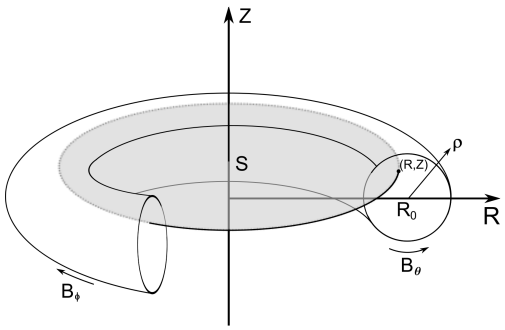

Figure 1. Coordinates (R, Z) and surface $\boldsymbol{S}$ used to define the poloidal magnetic flux $\psi(R, Z)$.

factor is basically scaling as the ratio of the normalized radius to the poloidal magnetic flux gradient, controlling this latter variable allows controlling the safety factor profile, which is our main objective. This is a challenging problem for several reasons:

- the evolution of the q-profile is governed by the resistive diffusion of the magnetic flux, which is a parabolic equation with spatially-distributed rapidly time-varying coefficients that depend on the solution of another partial differential equation related to heat transport;
- the control action is distributed in the spatial domain but nonlinear constraints are imposed on its shape (with only a few engineering parameters being available for control, strong restrictions on the admissible shape are imposed);
- important uncertainties exist in most measurements, estimations and models;
- nonlinear source terms appear in the evolution equation (in particular the bootstrap current).

The problem of poloidal magnetic flux profile control is closely related, via the Maxwell equations, to the control of plasma current profile. Some previous works show the possibility of controlling profile shape parameters, for instance on Tore Supra: [8], where the current profile shape is characterized by the internal inductance and the central safety factor value and experimental results are presented; and [9], where the control of the width of the lower hybrid power deposition profile is shown and experimentally validated. Also, [10] proposes a discrete real-time control of the steady-state q-profile, considering some possible operating modes. Other works consider the distributed nature of the system and use discretized linear models identified around experimental operating point. An example of such work can be found in [11], where a model based on a Galerkin projection was used to control multiple profiles in JET; in [12], where a reduced order model is used to control some points in the q-profile and in [13], where the applicability of these identification and integrated control methods to various tokamaks is presented.

Specific contributions from the automatic control research community have also started to appear, dealing with simplified control-oriented models that retain the distributed nature of the system. An example is [14] and related works, where an infinite-dimensional model, described by partial differential equations (PDEs), is used to construct an extremum-seeking controller for the current profile, considering fixed shape profiles for the current deposited by the RF antennas and for the

diffusivity coefficients. Other PDE-control approaches, related to Tore Supra, can also be mentioned: [15], where sum-of-square polynomials are used to construct a Lyapunov function considering constant diffusivity coefficients; [16], where a sliding-mode controller was designed for the infinite-dimensional system, considering time-invariant diffusivity coefficients; [17], where a polytopic linear parameter-varying approach is used to build a common Lyapunov function guaranteeing stability of the discretized system with time-varying diffusivity profiles and finally [18], where an infinite dimensional Lyapunov function is constructed to guarantee the stability and robustness of the controlled system, considering distributed time-varying diffusivity coefficients as well as non-linear shape constraints in the actuation profiles due to the use of two engineering parameters (the power and the parallel refraction index of the lower-hybrid antennas) to control the safety factor profile.

Some references dealing with the control of parabolic partial differential equations (in particular, diffusion equations) can be mentioned as: [19] and, more recently [20], studying controllability aspects of semilinear heat equations; [21] and subsequent papers where a Lyapunov function is used on a heat equation with unknown destabilizing parameters; [22], where the control of diffusion-convection equations with constant diffusion and distributed convection coefficients is treated; [23], where the case of distributed (but not time-varying) diffusion coefficients is studied; and [24], where constant diffusion coefficients and distributed time-varying convection coefficients are considered.

The main contributions of this paper are:

- the use of a physically relevant control-oriented infinite-dimensional model (see [6]) for the design of a distributed control law to track the gradient of the magnetic flux profile (and consequently the q-profile) by means of LH current drive, with particular care given to time-varying effects and possible extension to arbitrary non-inductive current sources;
- building upon [18] and [25], the consideration of time varying diffusivity coefficient profiles in the control design, guaranteeing the stability of the system and its robustness with respect to several common sources of errors and unmodeled dynamics;
- the inclusion of previously neglected couplings between the total plasma current control and the magnetic flux profile control;
- real-time optimization that includes the nonlinear constraints imposed by the current deposit profiles while preserving the theoretical stability and robustness guarantees;
- the validation of the proposed control approach using the METIS code [26].

The main advantages of the chosen Lyapunov approach for this problem are:

- no assumption of fixed shape of the control inputs is required (this allows to consider, for example, the shift of the location of the peak current density deposited by the LH antenna when changing the engineering parameters);
- no assumption of fixed or slowly time-varying shape of the diffusivity profiles is made (this allows to consider the fast time-variant nature of the temperature profile and the changes in its shape when heating actuators are used);
- since it is not based on an identified linear model, the validity domain for the analysis is larger (as illustrated in the simulation results);

- the extensive robustness analysis presented in [18] provides a clear idea of the impact of the tuning parameters and the profile estimation errors on the behaviour and stability of the system;
- the resulting control law is easy to implement and requires little online computing ressources (ideal for real-time implementation);
- the resulting control law can be easily extended to include other non-inductive actuators (e.g. Electron Cyclotron Current Drive antennas).

All the numerical simulations were performed using Tore Supra parameters, as this work aims to assess the capabilities of this novel safety factor control approach before experimental implementation. Tore supra was chosen for its capability to produce long lasting plasma discharges, offering a unique opportunity to develop and test plasma safety factor profile control schemes on relevant timescales. The extension of these results to other tokamaks will be discussed.

In Section 2, the simplified, infinite-dimensional, control-oriented model (based on [6]) used for the control design is presented, along with the main related physical hypotheses. The couplings between the distributed system and the finite-dimensional subsystem regulating the total plasma current are formulated and an appropriate change of variables suitable for the stability analysis is introduced. In Section 3 the Lyapunov-based control approach is shown and discussed. In Section 4, the proposed control law is implemented and evaluated for Tore Supra with METIS.

2. Reference Model

In this section, we couple a simplified 1D model of poloidal magnetic flux diffussion with a 0D model of the time-evolution of the total plasma current via the external boundary condition of the 1D model.

2.1. Poloidal (1D) Magnetic Flux Transport Model

In this article, the q-profile regulation is done by controlling the gradient of the poloidal magnetic flux profile.

For the development of a suitable control law, a simplified model for the magnetic flux profile ψ in its one-dimensional representation is considered as in [27]:

$$\frac{\partial \psi}{\partial t} = \frac{\eta_{\parallel} C_2}{\mu_0 C_3} \frac{\partial^2 \psi}{\partial \rho^2} + \frac{\eta_{\parallel} \rho}{\mu_0 C_3^2} \frac{\partial}{\partial \rho} \left(\frac{C_2 C_3}{\rho} \right) \frac{\partial \psi}{\partial \rho} + \frac{\eta_{\parallel} V_\rho B_{\phi_0}}{F C_3} j_{ni} \tag{1}$$

where $\rho \doteq \sqrt{\frac{\phi}{\pi B_{\phi_0}}}$ is an equivalent radius indexing the magnetic surfaces, ϕ is the toroidal magnetic flux, B_{ϕ_0} is the toroidal magnetic field at the geometric center of the plasma, $\eta_{\parallel}$ is the parallel resistivity of the plasma, j_{ni} represents the current density profile generated by non-inductive current sources (source term), μ_0 is the permeability of free space, F is the diamagnetic function, C_2 and C_3 are geometric coefficients and V_ρ is the derivative of the plasma volume with respect to the spatial variable ρ. Some other variable definitions are given in Table 1.

Neglecting the diamagnetic effect caused by poloidal currents and using a cylindrical approximation of the plasma geometry ($\rho << R_0$, where R_0 is the major plasma radius) the coefficients in (1) simplify as follows:

$$F \approx R_0 B_{\phi_0}, \quad C_2 = C_3 = 4\pi^2 \frac{\rho}{R_0}, \quad V_\rho = 4\pi^2 \rho R_0 \tag{2}$$

Variables	*Description*	*Units*
ψ	Poloidal magnetic flux profile	Tm^2
ϕ	Toroidal magnetic flux profile	Tm^2
q	Safety factor profile $q \doteq d\phi/d\psi$	
R_0	Location of the magnetic center	m
B_{ϕ_0}	Toroidal magnetic field at the center	T
ρ	Equivalent radius of the magnetic surfaces	m
a	Location of the last closed magnetic surface (minor radius of the torus)	m
r	Normalized spatial variable $r \doteq \rho/a$	
t	Time	s
V	Plasma Volume	m^3
F	Diamagnetic Function	Tm
C_2, C_3	Geometric coefficients	
$\eta_\parallel$	Parallel resistivity	Ωm
η	Normalized diffusivity coefficient $\eta_\parallel/\mu_0 a^2$	s^{-1}
μ_0	Permeability of free space: $4\pi \times 10^{-7}$	Hm^{-1}
$\overline{n}$	Electron average density	m^{-3}
j_{ni}	Non-inductive effective current density	Am^{-2}
j	Normalized non-inductive effective current density $\mu_0 a^2 R_0 j_{ni}$	Tm^2
I_p	Total plasma current	A
V_{loop}	Toroidal loop voltage	V
η_{lh}	LH current drive efficiency	$Am^{-2}W^{-1}$
P_{lh}	Lower Hybrid antenna power	W
$N_\parallel$	Hybrid wave parallel refractive index	
I_Ω	Ohmic current	A
V_Ω	Ohmic voltage	V

Table 1. Variable definition

Defining a normalized spatial variable $r = \frac{\varrho}{a}$, where a (assumed constant) is the equivalent (minor) radius of the last closed magnetic surface, the simplified model is obtained, as [6, 7]:

$$\frac{\partial \psi}{\partial t}(r,t) = \frac{\eta_\parallel(r,t)}{\mu_0 a^2}\left(\frac{\partial^2 \psi}{\partial r^2} + \frac{1}{r}\frac{\partial \psi}{\partial r}\right) + \eta_\parallel(r,t) R_0 j_{ni}(r,t) \tag{3}$$

with the boundary conditions $\partial\psi/\partial r(0,t) = 0$ and $\partial\psi/\partial r(1,t) = -R_0\mu_0 I_p(t)/(2\pi)$ or $\partial\psi/\partial t(1,t) = -V_{loop}(t)/(2\pi)$ where I_p is the total plasma current and V_{loop} is the toroidal loop voltage, with initial condition:

$$\psi(r,t_0) = a^2 B_{\phi_0}\int_r^1 \frac{s}{q(s,t_0)}ds + \psi(1,t_0) \tag{4}$$

For the purposes of this article, j_{ni} is considered as having two main components:

- the auto-induced bootstrap current j_{bs} (produced by trapped particles in the "banana" regime);
- the LHCD (*Lower Hybrid Current Drive*) current deposit j_{lh}.

Using the previous hypotheses and approximating the toroidal magnetic flux as $\phi(\rho,t) \approx -B_{\phi_0} a^2 \rho^2/2$ (see [6]), we can consider the safety factor profile to be related to the poloidal magnetic flux as $q(\rho,t) = -B_{\phi_0} a^2 \rho / \psi_\rho$.

Normalizing the constants in (3) by defining $\eta \doteq \eta_\parallel/\mu_0 a^2$ and $j \doteq \mu_0 a^2 R_0 j_{ni}$ to simplify notations, an equilibrium $\left(\overline{\psi}, \overline{j}, \overline{I}_p, \overline{\eta}\right)$ is defined as the stationary solution of:

$$0 = \left[\frac{\overline{\eta}}{r}\left[r\overline{\psi}_r\right]_r\right]_r + \left[\overline{\eta}\overline{j}\right]_r \forall r \in (0,1) \tag{5}$$

with boundary conditions $\overline{\psi}_r(0) = 0$ and $\overline{\psi}_r(1) = -R_0\mu_0\overline{I}_p/(2\pi)$; where, for any function ξ depending on the independent variables r and t, ξ_r and ξ_t are used to denote $\frac{\partial}{\partial r}\xi$ and $\frac{\partial}{\partial t}\xi$ respectively. These equations imply that the time-derivative of ψ is constant over the spatial interval $[0,1]$ (and, in general, different from zero when $V_{loop} \neq 0$).

Around this equilibrium, neglecting the nonlinear dependence of the bootstrap current on the state, the dynamics of the system is given by:

$$\tilde{\psi}_t = \frac{\eta}{r}\left[r\tilde{\psi}_r\right]_r + \eta\tilde{j},\ \forall (r,t) \in (0,1)\times[0,T) \tag{6}$$

with boundary conditions $\tilde{\psi}_r(0,t) = 0$ $\tilde{\psi}_r(1,t) = -R_0\mu_0\tilde{I}_p(t)/(2\pi)$ and initial condition $\tilde{\psi}(r,0) = \tilde{\psi}_0(r)$; and where the dependence of $\tilde{\psi}$, $\tilde{j}$ and η on (r,t) is implicit; $\tilde{I}_p \doteq I_p - \overline{I}_p$ and $0 < T \leq +\infty$ is the time horizon. For all variables, a tilde represents the difference between the actual value and the equilibrium ($\tilde{\xi} \doteq \xi - \overline{\xi}$).

Our focus is on the evolution of $z \doteq \partial\tilde{\psi}/\partial r$, with input $u \doteq \tilde{j}$, as defined by:

$$z_t(r,t) = \left[\frac{\eta(r,t)}{r}\left[rz(r,t)\right]_r\right]_r + \left[\eta(r,t)u(r,t)\right]_r,\ \forall (r,t) \in (0,1)\times[0,T) \tag{7}$$

with Dirichlet boundary conditions:

$$\begin{aligned} z(0,t) &= 0 \\ z(1,t) &= -\frac{R_0\mu_0\tilde{I}_p(t)}{2\pi} \end{aligned} \tag{8}$$

and initial condition:

$$z(r,0) = z_0(r) \tag{9}$$

where $z_0 \doteq \partial\tilde{\psi}_0/\partial r$.

2.2. 0D total plasma current dynamic model

Assuming $I_{lh} = \eta_{lh}P_{lh}/(R_0\overline{n})$ (where η_{lh} is the efficiency of the LH current drive, P_{lh} is the power delivered by the LH antennas and $\overline{n}$ is the electron line average density) and using a transformer model as in [28], the evolution of $\tilde{I}_p \doteq I_p - \overline{I}_p$ around an equilibrium $(\overline{I}_p, \overline{P}_{lh}, \overline{N}_\parallel, \overline{V}_\Omega, \overline{I}_\Omega)$ can be considered, neglecting the variations of bootstrap current, as given by:

$$\begin{bmatrix} L_p & M \\ M & L_\Omega \end{bmatrix}\begin{bmatrix} \dot{\tilde{I}}_p \\ \dot{\tilde{I}}_\Omega \end{bmatrix} = \begin{bmatrix} -R_p & 0 \\ 0 & -R_\Omega \end{bmatrix}\begin{bmatrix} \tilde{I}_p \\ \tilde{I}_\Omega \end{bmatrix} + \begin{bmatrix} \frac{\eta_{lh}R_p}{\overline{n}R_0} & 0 \\ 0 & 1 \end{bmatrix}\begin{bmatrix} \tilde{P}_{lh} \\ \tilde{V}_\Omega \end{bmatrix} \tag{10}$$

with initial condition $\tilde{I}_p(0) = \tilde{I}_\Omega(0) = 0$.

Let us define the matrices A, B and D as follows:

$$A = \begin{bmatrix} -\frac{L_\Omega R_p}{L_p L_\Omega - M^2} & \frac{M R_\Omega}{L_p L_\Omega - M^2} & 0 \\ \frac{M R_p}{L_p L_\Omega - M^2} & -\frac{L_p R_\Omega}{L_p L_\Omega - M^2} & 0 \\ -1 & 0 & 0 \end{bmatrix}, B = \begin{bmatrix} -\frac{M}{L_p L_\Omega - M^2} \\ \frac{L_p}{L_p L_\Omega - M^2} \\ 0 \end{bmatrix},$$

$$D = \begin{bmatrix} \frac{L_\Omega \eta_{lh} R_p}{(L_p L_\Omega - M^2)\overline{n} R_0} \\ -\frac{M \eta_{lh} R_p}{(L_p L_\Omega - M^2)\overline{n} R_0} \\ 0 \end{bmatrix}$$

Equation (10) can be rewritten, around the equilibrium and adding an integrator to reject constant disturbances, as:

$$\dot{\zeta} = A\zeta + B\tilde{V}_\Omega + D\tilde{P}_{lh} \tag{11}$$

where $\zeta \doteq \begin{bmatrix} \tilde{I}_p & \tilde{I}_\Omega & E \end{bmatrix}^T$, and E is the integral of the tracking error of I_p.

For simplicity in the calculations and proofs, this article considers constant matrices A, B and C. A more advanced approach, using a linear parameter-varying (LPV) formulation (such as [17] for the total plasma current) can avoid this assumption to extend our results to the time-varying case.

Since $L_p L_\Omega - M^2 > 0$, matrix A has two eigenvalues with negative real parts (corresponding to the physical system) and one zero eigenvalue (corresponding to the integrator).

The second boundary condition in (8) can be written as:

$$z(1,t) = C\zeta \tag{12}$$

where $C \doteq \begin{bmatrix} -\frac{R_0 \mu_0}{2\pi} & 0 & 0 \end{bmatrix}$. The relation between the 0D and 1D models is concisely expressed in equations (10) and (12).

3. Feedback Control Approach

3.1. Control Problem

For a given reference q-profile, our aim is to ensure a proper tracking using both the LH antenna and poloidal coils. The main control problem can thus be stated as:

- To guarantee the exponential stability of the origin, in the topology of the L^2 norm, defined in the usual manner (see for instance [29]), of solutions of system (7)-(9), with boundary condition given by (10)-(12), both in open-loop (with $u = 0$) and by closing the loop with a controlled input $u(\cdot, t)$ corresponding to a change in non-inductive current actuation (in particular LH current);
- to be able to adjust (in particular, to accelerate) the rate of convergence of the system using the controlled input;
- to guarantee the stability of the system in presence of a large class of errors. In particular actuation errors, estimation/measurement errors and state disturbances have been considered in [18].

This problem is illustrated in Figure 2.

The chosen approach to solve this problem is the construction of a strict Lyapunov function. Using this Lyapunov function, a simple control law that guarantees the stability of the system and allows attenuating possible disturbances is presented, based on the results presented in [18].

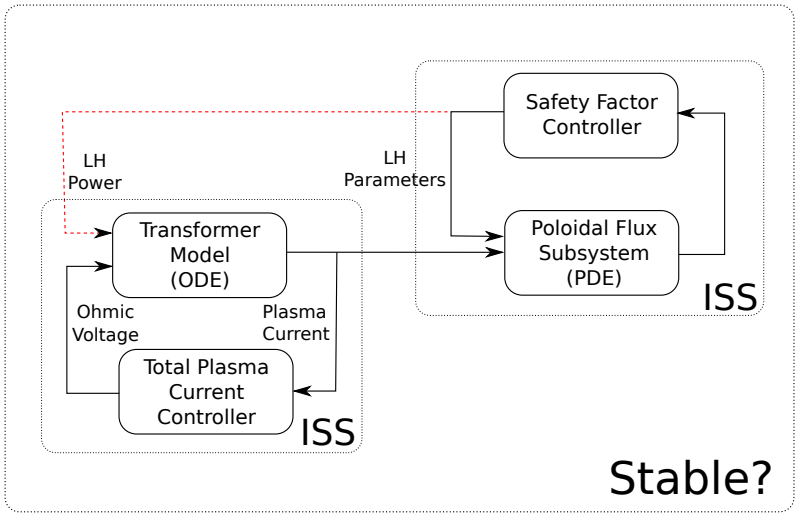

Figure 2. Diagram representing the coupling between the finite-dimensional and infinite-dimensional subsystems and the main control problem.

3.2. Proposed Lyapunov Function

Let us consider the following candidate Lyapunov function:

$$\begin{aligned} V &= V_1 + V_2 \\ V_1 &= \frac{1}{2}\int_0^1 f(r) z^2(r,t) dr \\ V_2 &= \frac{1}{2}\zeta^T P \zeta \end{aligned} \tag{13}$$

with $f : [0,1] \to [\varepsilon, \infty)$ a twice continuously differentiable positive function and $P = P^T \in \mathbb{R}^{2\times 2}$ a symmetric positive definite matrix.

Remark 3.1 *The weighting function $f(r)$ is computed to guarantee the strict decrease of the Lyapunov function. A constant $f(r)$ is not, in general, enough to guarantee this decrease for all admissible values of the resistivity profile.*

Theorem 3.2 *If the following two conditions are satisfied:*

(i) there exists a twice continuously differentiable positive weight $f : [0,1] \to [\varepsilon, \infty)$ as defined in (13) such that the function $V_1(z)$ is a strict Lyapunov function for system (7)-(9) with homogeneous boundary conditions, verifying for some positive constant α_1, $\dot{V}_1 \leq -\alpha_1 V_1$;

(ii) an independent control loop regulates the total plasma current while ensuring, for some symmetric positive definite matrix $P \in \mathbb{R}^{3\times 3}$, some matrix $K \in \mathbb{R}^{1\times 3}$ and some positive constant α_2:

$$P[A + BK + \alpha_2 \boldsymbol{I}_3] - \frac{R_0^2 \mu_0^2}{8\pi^2}\left(f(1) + f'(1)\right)\eta(1,t)\boldsymbol{I}_3 \prec 0 \tag{14}$$

where $\cdot \prec 0$ denotes the negative definiteness of a square matrix, $\boldsymbol{I_3}$ is the 3×3 identity matrix, f' represents $\frac{d}{dr}f$;

then the function $V(z,\zeta)$ is a strict Lyapunov function for the interconnected system, satisfying for some positive constant γ:

$$\dot{V} \leq -\min\{\alpha_1,\alpha_2\}V(z,\zeta) + \gamma \sup_{0\leq\tau\leq t} |\tilde{P}_{lh}(\tau)|, \forall t \in [0,T) \tag{15}$$

The proof of this result is given in Appendix A.

Remark 3.3 *It can be shown, based on the previous theorem, that for constant values of $\tilde{P}_{lh}$ the exponential convergence of the interconnected system can be achieved with the same rate as that of the infinite-dimensional system if the rate of exponential convergence of the plasma current control is faster by at least $-R_0^2\mu_0^2/(8\pi^2)\,(f(1)+f'(1))\,\eta(1,t)$ than that of the magnetic flux profile. This term accounts for the impact of the coupling between the 0D (finite-dimensional) plasma circuit equation and the 1D (infinite-dimensional) magnetic-flux diffusion equation by means of the total plasma current (boundary condition). Even if this condition is not verified, the error in the infinite-dimensional state will always remain bounded as long as $\tilde{P}_{lh}$ remains bounded and, furthermore, this error will be inversely proportional to the rate of convergence of this subsystem (α_2), which is why a fast convergence of the total plasma control is desirable.*

For the rest of this article, condition (14) is assumed to be verified for some $\alpha_2 >> \alpha_1$, and therefore $\alpha = \alpha_1$ and we can focus only on the evolution of the infinite dimensional subsystem. This assumption is physically justified by the fact that Ohmic current can be generated at a much faster time scale than that of the poloidal magnetic flux diffusion.

3.3. Control Law

Based on the constructed Lyapunov function and particularly on equation (A.8) (in the Appendix), a feedback controller was designed, as detailed in [18], based on a constrained optimization problem. This controller attempts to maximize the rate convergence of the Lyapunov function to zero while respecting the actuator limitations (the cost function is the control-dependent term appearing in the upper bound of the time-derivative of the Lyapunov function given by equation (A.8)).

At each time step, a couple of antenna parameters $(P_{lh}^*, N_\parallel^*)$ is chosen as follows:

$$(P_{lh}^*, N_\parallel^*) = \arg \min_{(P_{lh},N_\parallel)\in\mathcal{U}} \int_0^1 f(r)\left[\eta u(P_{lh},N_\parallel)\right]_r z dr \tag{16}$$

thus maximizing the convergence rate with an admissible control action, and subject to the constraint:

$$\int_0^1 f(r)\left[\eta u(P_{lh}^*,N_\parallel^*)\right]_r z dr \leq 0 \tag{17}$$

to guarantee preserving the stability of the system. Here $\mathcal{U} \doteq [P_{lh,min}, P_{lh,max}] \times [N_{\parallel,min}, N_{\parallel,max}]$ is the set of admissible values for the engineering parameters of the LH antennas (P_{lh} is the LH power and $N_\parallel$ the Hybrid wave parallel refractive index). It is important to note that a feasible starting point for the optimization problem always exists (it corresponds to setting u to zero, and thus keeping the open-loop response of the system). For more details, see [18].

The constraints imposed by the achievable shapes of the LH current deposit are taken into account in the shape of the u function in the problem. Other constraints

Type of error	*Type of expected upper bound for the L^2 norm of z*
Unmodeled dynamics (w)	$ce^{-\alpha t}\|z_0\|_{L^2} + c\int_0^t e^{-\alpha(t-\tau)}\|w(\cdot,\tau)\|_{L^2}d\tau$
Actuation error (ε^u)	$ce^{-\alpha t}\|z_0\|_{L^2} + c_2\int_0^t e^{-\alpha(t-\tau)}\|\varepsilon^u(\cdot,\tau)\|_{H^1}d\tau$
Profile estimation error (ε^z)	$ce^{-\alpha t}\|z_0\|_{L^2} + c_3\int_0^t e^{-\alpha(t-\tau)}\|\varepsilon^z(\cdot,\tau)\|_{L^2}d\tau$
Resistivity estimation error (ε^η)	$ce^{-\alpha_2 t}\|z_0\|_{L^2}$

Table 2. Expected ISS gain bounds in a simple case, from [18]

(such as a variation rate on the engineering parameters) can also be taken into consideration while solving this problem.

Remark 3.4 *The robustness of the proposed scheme with respect to a variety of disturbances and errors was studied in detail in [18] and extended to the case where there is a non-vanishing disturbance in the boundary condition in [25].*

In particular, Input-to-State Stability (ISS) results were obtained with respect to the considered disturbances. Input-to-State Stability means to guarantee a bounded gain (in some appropriate sense) between the inputs of the system (in this case the errors in estimations of the poloidal magnetic flux profile and resistivity and the disturbances produced by the non-homogeneous boundary conditions and actuation errors) and the controlled output. For a detailed account of ISS results in the finite-dimensional case, see [30].

A schematic representation of the ISS concept is shown in Figure 3. An example of typical trajectories in ISS systems are shown for the Open-Loop (O.L.) and Closed-Loop (C.L.) cases. It can be seen that, in the presence of disturbances, the system does not converge to zero, but the error remains bounded. The feedback control usually seeks to attenuate the effect of these disturbances. The expected robustness results are provided in Table 2, which summarizes the results presented in [18]. To interpret this table adequately, the errors should be considered to affect the evolution of the system according to the following equation:

$$z_t = \left[\frac{\eta}{r}\left[rz\right]_r\right]_r + \left[\eta(u(\hat{\eta},\hat{z}) - \varepsilon^u)\right]_r + w \tag{18}$$

with the control action u being a function of the estimations of z and η ($\hat{z} \doteq z - \varepsilon^z$ and $\hat{\eta} \doteq \eta - \varepsilon^\eta$, respectively) and w being a state disturbance that can represent unmodeled dynamics.

Remark 3.5 *The constant c appearing in Table 2 arises from a change in norms in the L^2 space; the constant c_2 is determined by the bounds on the resistivity and its spatial derivative; the constant c_3 depends on the "gain" of the controller (once the constraints are satisfied); the constant α is the unactuated rate of convergence of the coupled system; and finally the constant α_2 is a function of the gain of the controller and the bounds on the error of estimation of η and its spatial derivative (for small enough estimation errors, the system remains exponentially stable). For more details, see [18].*

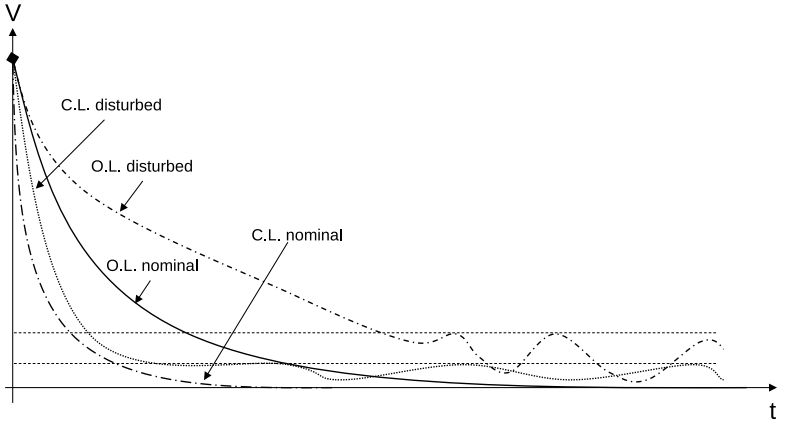

Figure 3. Schematic depiction of the Input to State Stability property and closed-loop improvements.

4. Application

4.1. Simulation Scheme

Although rapid simulations using the simplified model described in [6] were used in the early stages of controller development for tuning purposes, the proposed scheme is validated on a more complex simulation scheme. The Matlab/Simulink interface of the METIS code developed by the french CEA [26] was included in a flexible platform, developed to easily simulate the Tokamak evolution under different assumptions (e.g.: prescribed total plasma current vs. independent control loop using V_Ω) and different actuator models (such as the LH current deposit profile). This platform includes a controller subsystem, a local plasma current control loop and the METIS interface.

The METIS code solves the full version of the resistive diffusion equation, equivalent to (1) (without the simplifying hypotheses made for the control formulation), as presented in [7], but on a 21-point grid. It computes the MHD equilibrium (used to index the isoflux surfaces) using a fast solver based on moments of the Grad-Shafranov equation, which is not taken into account in the control-oriented model. The shapes of the current sources are based on simplified analytical formulations (unlike the functions used for the optimization, which are based on scaling laws as in [6]). The temperature profile (required to compute the resistivity profile) is computed solving time-independent transport equations and using a 0D solver for computing the energy content of the plasma (this is the main difference with respect to CRONOS, which also solves the temperature transport equation). For more details, see [26].

4.2. Closed-loop Tracking with Approximated Equilibrium $(\overline{\psi}, \overline{j}, \overline{I}_p, \overline{\eta})$

4.2.1. General Description

The presented simulation results are based on general parameters of Tore Supra shot TS-31463, but with a much larger variation range for P_{lh} and $N_\parallel$ (in order to better illustrate the robustness of the controller when the equilibrium is poorly known

or when large variations around the known equilibrium are needed). The shot was simulated with METIS.

The chosen inputs to the controller were the spatial derivative of the poloidal magnetic flux profile, as well as a reference profile (which could be generated from a reference safety factor profile), and an estimate of the parallel resistivity profile. Although the poloidal magnetic flux profile (considered available in Tore Supra from Equinox reconstructions in real time [31]) and parallel resistivity may not be perfectly known, the robustness of Lyapunov-based controllers with respect to estimation errors in both profiles has already been studied in [18] and summarized in Table 2. Plasma parameter estimation could also be done using other methods, such as those found in [32]. The controller outputs were chosen to be $N_{\|}$ and P_{lh}.

Since, in practical applications, the full set of available or desired equilibria might not be easily known (in particular due to nonlinearities such as the bootstrap current and couplings with the temperature equation), a single approximated equilibrium point was estimated, simulating in METIS the Open-Loop behaviour of the system for fixed values of the $N_{\|}$ and P_{lh} inputs. The ability of the controller to reach or approach other desired profiles and stabilize the system around the corresponding equilibrium was tested.

The ramp-up phase of the simulated shot was done in open-loop (as far as $N_{\|}$ and P_{lh} are concerned, using only an independent control loop for I_p) based on TS-31463. The controller was activated at $t = 9$ `s`. Since Real-Time implementation is desired, an offline computation was done to construct a table with profiles of LH current deposit as a function of the input parameters to the controller using scaling laws as in [6]. The real-time optimization algorithm can then perform a constrained gradient-descent, using the estimated values of the resistivity profile and the state, and find a suitable control action in less than two hundred microseconds (using MATLAB functions and an Intel processor running at 2.43 `GHz`).

The global parameters during the flat-top phase are: constant total plasma current of 580 `KA`; constant line-average electron density of 14.5×10^{18} $\mathtt{m}^{-2}$; non-inductive heating and current drive using LHCD with $P_{lh} \in [0.17, 3.5]$ `MW` and $N_{\|} \in [1.70, 2.30]$; and constant toroidal magnetic field at the center of the plasma of 3.69 `T`.

4.2.2. First case: Independent I_p control, large variations of P_{lh}, temperature profile disturbed by ICRH heating. This test case was chosen to illustrate the robustness of the controller under non-ideal circumstances:

- the total plasma current I_p is independently controlled using the poloidal field coils. Since it is no longer considered to be perfectly followed, it becomes a source of disturbances in the plasma edge (boundary condition of the partial differential equation);
- during the shot, reference profiles are chosen far from the equilibrium used for the controller design (corresponding to values of P_{lh} and $N_{\|}$ of 2.76 `MW` and 2, respectively). This highlights the contribution of non-linear terms in the equations that were neglected near the equilibrium;
- a disturbance in the temperature profile is introduced in the form of 1.5 `MW` of power from ion-cyclotron radio heating (ICRH) antennas, which cannot be compensated with the LH actuator, thus rendering the target q-profile inaccessible to the controller;

- the model given to the controller for the LH current deposit is based on a gaussian profile approximation with parameters determined by scaling laws, as described in [6]. This does not correspond to the internal METIS model (where, even though the LH efficiency is calculated using scaling laws depending on plasma and wave parameters [33], the shape is based on Landau absorption, accessibility and caustics [26]);
- the general parameters were taken from experimental measurements of shot TS-31463 and therefore introduce measurement noise to all the variables used to compute the control action.

The tracking of the desired q-profiles and the engineering parameters prescribed by the controller for the LH antenna are presented in Figure 4. First, Figure 4 (a) depicts the evolution of the safety factor at six points (corresponding to $r = 0$, 0.1, 0.2, 0.3, 0.5 and 0.8) during the control window ($9\ \mathtt{s} \leq t \leq 23\ \mathtt{s}$). The solid lines represent the simulated evolution of the closed-loop system while the dashed lines represent the reference values given to the controller (calculated from an open-loop simulation without disturbances). It can be seen that the tracking is satisfactory regardless of the radial position. For t between 13.4 `s` and 16.6 `s` (and again after 22.6 `s`) the tracking error does not converge to zero, which corresponds to the introduction of a disturbance caused by ICRH. Nevertheless, the system remains stable and the error small, even though the reference profile is no longer achievable. As soon as the disturbance is removed, the tracking errors are promptly reduced. No undershoot or overshoot is noticeable in the tracking of the reference profile (which is a desirable property to avoid triggering unwanted magnetohydrodynamic modes). There is a lag between the reference profile and the response of the system, which is to be expected since: (a) an error between both signals has to appear before the feedback controller can act, and (b) the rate at which the gradient-descent optimization algorithm is allowed to modify the controlled inputs is limited to filter out noise and to prevent sudden changes to the engineering parameters of the LH antennas. Figure 4 (b) presents the evolution of the engineering parameters used to track the safety factor profile. In solid lines, the parameters $N_{\|}$ and P_{lh} set by the controller are shown. The parameters used to construct the reference profile are depicted with dashed lines. These figures show that the controller is able to properly reconstruct the engineering parameters required to obtain the desired safety factor (with the saturation on the rate of change of the parameters revealed by the constant slope during big changes in reference). A mark at the beginning of the control action shows the approximated equilibrium around which the controller was designed. The dashed-dotted line shows the ICRH power injected into the system (only applied to the closed-loop system and not taken into account for the reference generation, as would be the case with unexpected disturbances encountered during actual tokamak operation). These results show the robustness of the proposed Lyapunov-based approach to changes in operating conditions. Although the value of $N_{\|}$ is modified during closed-loop operation, the changes are very small. Finally, even though there is some overshoot in the control parameters chosen by the controller, as mentioned before, these do not cause overshoots in the tracked safety factor profiles.

The tracking of the total plasma current and the resulting loop voltage are depicted in Figure 5. Figure 5 (a) shows the plasma current tracking efficiency of a well-tuned proportional-integral (PI) controller despite constant disturbances (in this case, induced by changes in LH current). During the shot, the current driven by

the LH antenna varies considerably (since the LH power is driven between 3 and 1 MW). Nevertheless, the tracking error in the plasma current remains small and goes to zero once the safety factor profile stabilizes. This error acts as a small disturbance in the boundary condition of the partial differential equation that eventually vanishes. The resulting loop voltage can be seen in Figure 5 (b). This figure shows the capability of the controller to handle both the non-inductive current drives and the addition of inductive current.

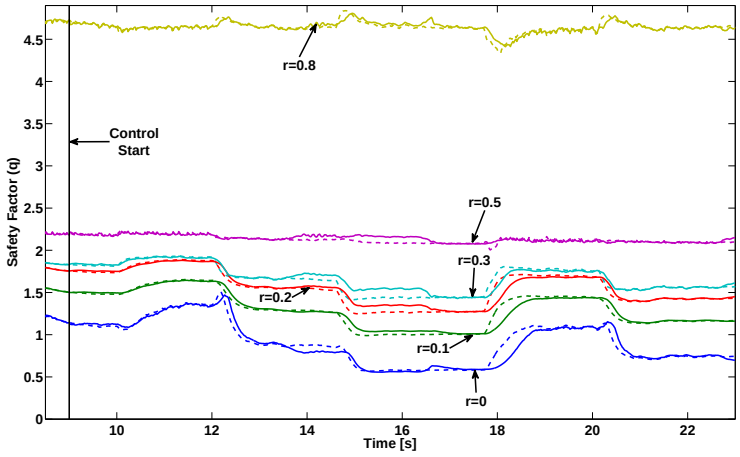

(a) Tracking of the safety factor profile. Dashed line: reference q value; full line: obtained q value.

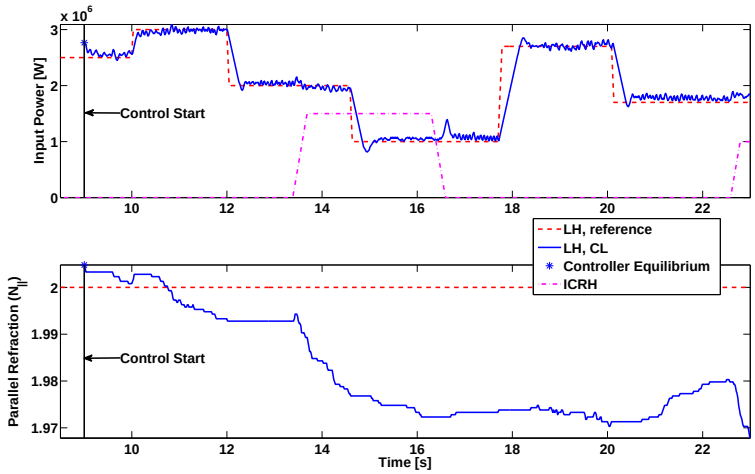

(b) Controller action and ICRH disturbance.

Figure 4. Safety factor profile tracking and radio-frequency antenna control parameter evolution.

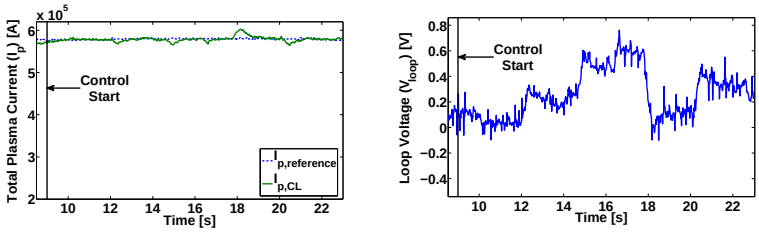

(a) Tracking of the total plasma current. (b) Resulting V_{loop} due to I_p tracking.

Figure 5. Total plasma current evolution and corresponding loop voltage.

4.2.3. Second case: Independent I_p control, large variations of $N_\parallel$, temperature profile disturbed by ICRH heating. The purpose of this second test case is to show the versatility of the controller with respect to different available control parameters. The general shot conditions are the same as those chosen for the previous example. Nevertheless, the safety factor reference profile is generated by changing the $N_\parallel$ parameter between 1.75 and 2.25 while P_{lh} is held constant at 2.7 MW. The results of the simulation can be seen in Figures 6 and 7. Although the safety factor reference is different from that used in the previous example (for instance, the variations of q at $r = 0.5$ are much more important in the second simulation, while the central safety factor varies less), the tracking remains satisfactory, as seen in Figure 6 (a). As in the previous example, the tracking error does not converge to zero when the ICRH disturbance is introduced (between 13.4 s and 16.6 s, and after 22.6 s), yet the system remains stable and the error small. Figure 6 (b) shows a good reconstruction of the original engineering parameters used to generate the reference, except when the ICRH disturbance is present. The effect of the disturbance is attenuated by an offset in the equilibrium $N_\parallel$ values. As in the previous example, the overshoots present at some points in the control profile do not induce overshoots for the safety-factor tracking.

Figure 7 shows that the total plasma current tracking (boundary condition) is better than in the previous case, which is to be expected since the variations of LH power are much smaller. This has a direct impact on the tracking of the safety factor profile near the edge ($r = 0.8$ in Figure 6 (a)). Finally, Figure 7 (b) shows that the non-inductive control effort to maintain the prescribed total plasma current is smaller than in the previous case.

4.2.4. Third case: Independent I_p control, reference step, P_{lh} disturbance, temperature profile disturbed by ICRH heating. This last case was chosen to illustrate the interest of closing the loop for the system. The general conditions are the same as those in the first case. The objective is to stabilize the system and switch between two well-known equilibrium values (i.e. such that, without disturbances, the open-loop system will converge to the reference). In the first two cases, one of the main objectives was to illustrate the possibility of tracking references with imperfect knowledge of the actual equilibrium values. In this case, the objective is to compare the performance and disturbance rejection of the system in closed-loop and open-loop. Two different disturbances are applied to the system:

- a disturbance in the temperature profile is introduced as an additional 1.5 MW of power from ion-cyclotron radio heating (ICRH) antennas, which cannot be

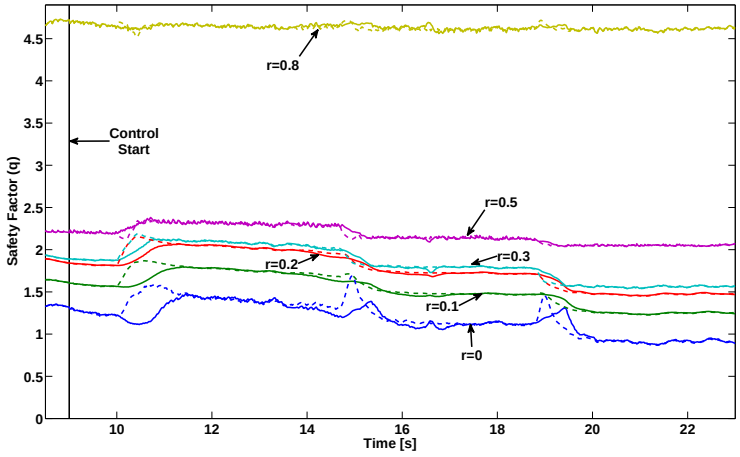

(a) Tracking of the safety factor profile. Dashed line: reference q value; full line: obtained q value.

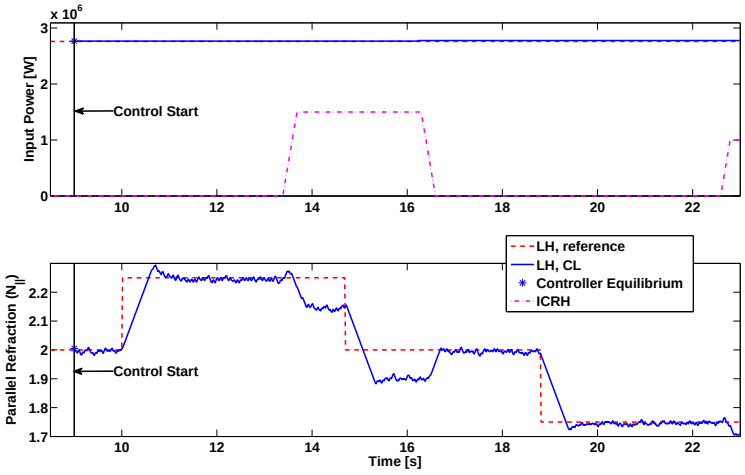

(b) Controller action and ICRH disturbance.

Figure 6. Safety factor profile tracking and radio-frequency antenna parameter evolution.

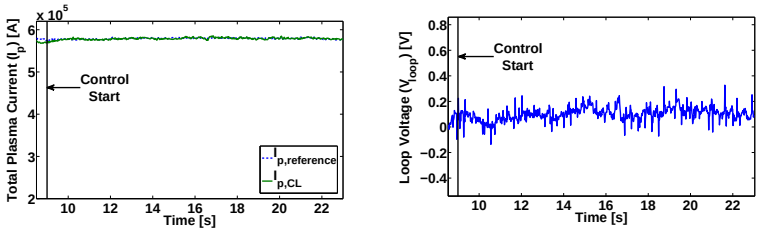

(a) Tracking of the total plasma current. (b) Resulting V_{loop} due to I_p tracking.

Figure 7. Total plasma current evolution and corresponding loop voltage.

compensated with the LH actuator, thus rendering the target q-profile inaccessible to the controller;

- a disturbance in the LH power applied to the system (vs. the one prescribed by the controller) of 1 MW (this can be compensated by increasing the LH actuation).

The results of the simulation can be seen in Figures 8 (a) and (b). It can be seen that, in the absence of disturbances, the closed-loop system behaves similarly to the open-loop one (albeit with small differences between 10 and 13 s). The ICRH disturbance is attenuated, particularly at values of r between 0.1 and 0.3 (where the control action is more present). Finally, the LH power disturbance is rejected by the controller, while the open-loop system converges to a safety factor profile far from the reference.

This simulation illustrates the interest of using a feedback control with respect to using an open-loop strategy only.

5. Conclusions and Perspectives

In this article, a control law was designed for the safety factor profile tracking in a tokamak, via the gradient of the poloidal magnetic flux. This control law is set using a physically-relevant simplified model. Based on specific simplifying assumptions, theoretical stability was guaranteed despite large classes of disturbances and actuation/estimation errors. The couplings between the 0D total plasma current control and the 1D magnetic flux profile evolution (via the boundary condition), as well as actuator saturations, were included in the theoretical developments.

The chosen non-inductive current actuator, based on Tore Supra capabilities, was the LH current drive. Nevertheless, the theoretical basis is independent from the actual form of the current deposit and the proposed controller design strategy can easily be applied using other non-inductive current sources (such as ECCD and neutral-beam injection). The controller was validated using the METIS code [26]. The tracking of the full safety-factor profile shows promising results as safety factors far from the estimated equilibrium could be adequately reached, with central safety factors varying both above and below the critical $q = 1$ value. The robustness of the proposed scheme with respect to unmodeled disturbances in the temperature profile was tested by heating the plasma with ICRH power.

The chosen controller solves a reduced online optimization problem and relies on some off-line calculations to run in real-time. The average time required by the control algorithm to compute the control values at each time step was under 160 μs (using using a Matlab® function running on a processor at 2.54 GHz), well below the simulation sampling time. Future experimental validation of the control scheme in Tore Supra is expected.

The proposed method is based on a first-principle driven approach that is, as such, applicable to any tokamak. To use these results on other tokamaks, a new weight for the presented Lyapunov function may be required. The heuristic procedure presented in [25] allows to compute such weights in a simple manner for relatively general resistivity profiles. If needed, the procedure used to prove the main result in [18] can be applied to the resistive diffusion equation without using the cylindrical hypothesis (the terms C_2, C_3, F and $1/\rho$ in equation (1) could be computed from a 2D MHD equilibrium).

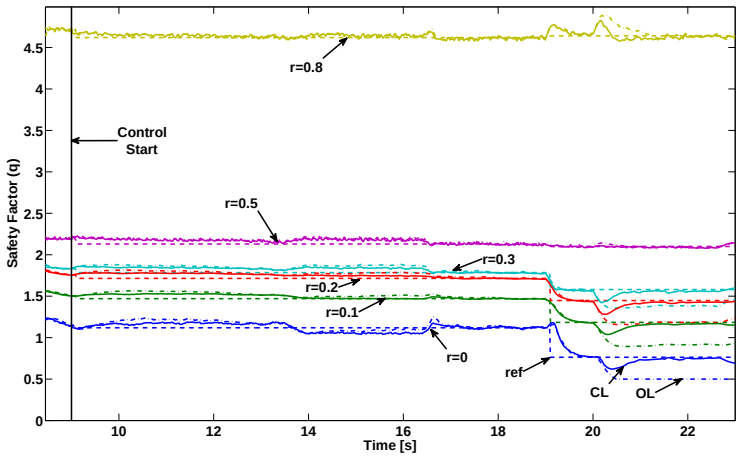

(a) Tracking of the safety factor profile. Dashed line: reference q value; full line: closed-loop q value; dash-dotted line: open-loop q value.

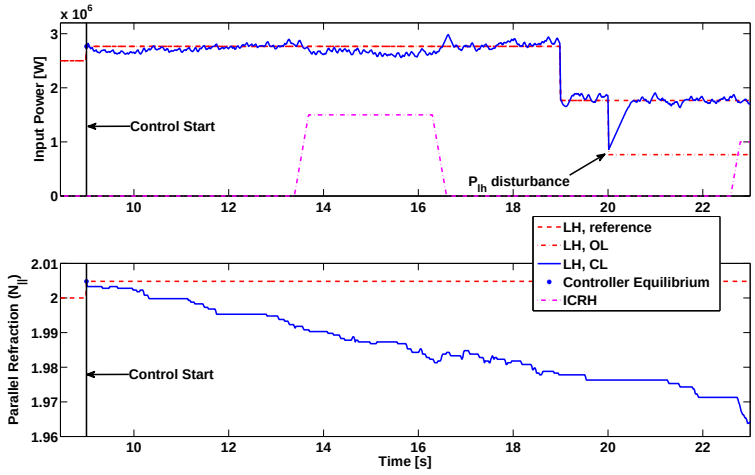

(b) Controller action and ICRH disturbance.

Figure 8. Safety factor profile tracking and radio-frequency antenna parameter evolution.

Acknowlegments

This work was carried out within the framework of the European Fusion Development Agreement and the French Research Federation for Fusion Studies. It is supported by the European Communities under the contract of Association between EURATOM and CEA. The views and opinions expressed herein do not necessarily reflect those of the European Commission. The research leading to these results has also received funding from the European Union Seventh Framework Programme [FP7/2007-2013] under grant agreement n^o 257462 HYCON2 Network of excellence.

Appendix A.

Proof of Theorem 3.1: Choosing an adequate function $f(r)$, for example the one proposed in [25], satisfying condition (i) of Theorem 3.2 and with $f(1)+f'(1)<0$ we have that, along the solution of (7)-(9):

$$\dot{V}_1 \leq -\alpha_1 V_1 + \int_0^1 f(r)[\eta u]_r z dr - \frac{1}{2}\left(f(1)+f'(1)\right)\eta(1,t)z^2(1,t) \quad \text{(A.1)}$$

where $\alpha_1 > 0$. This equation assumes the total current density, defined as in [27]:

$$j_T = -\frac{1}{\mu_0 R_0 a^2 r}\left(r\psi_{rr}+\psi_r\right) \quad \text{(A.2)}$$

to be zero on the last closed magnetic surface. It can be relaxed to assume only uniform boundedness and Lipschitz-continuity in time with some modifications, as presented in [25], albeit at the expense of more conservative bounds.

Differentiating V_2 along the solution of (11), we get:

$$\dot{V}_2 = \frac{1}{2}\zeta^T P\left[A\zeta + B\tilde{V}_\Omega + D\tilde{P}_{lh}\right] + \frac{1}{2}\left[\zeta^T A^T + \tilde{V}_\Omega^T B^T + \tilde{P}_{lh}^T D^T\right] P\zeta \quad \text{(A.3)}$$

Considering a control $\tilde{V}_\Omega$ of the form $K\zeta$, with K a row vector with three elements, the previous equation is equivalent to:

$$\dot{V}_2 = \zeta^T P\left[A+BK\right]\zeta + \zeta^T P\left[D\tilde{P}_{lh}\right] \quad \text{(A.4)}$$

If condition (ii) from Theorem 3.2 is satisfied, and from the choice of f, it implies that ζ remains bounded if $\tilde{P}_{lh}$ is bounded, and in particular that, for some positive constant γ:

$$\dot{V}_2 \leq -\alpha_2 V_2 + \gamma \sup_{0\leq\tau\leq t}|\tilde{P}_{lh}(\tau)|, \forall t \in [0,T) \quad \text{(A.5)}$$

Recalling the definition of the boundary condition (12), and from the definition of C, the derivative of V along the solution of the coupled system is given by:

$$\dot{V} \leq -\alpha_1 V_1 + \int_0^1 f(r)[\eta u]_r z dr - \frac{R_0^2\mu_0^2}{8\pi^2}\left(f(1)+f'(1)\right)\eta(1,t)\zeta^T\zeta + \dot{V}_2 \quad \text{(A.6)}$$

and hence:

$$\dot{V} \leq -\alpha_1 V_1 + \int_0^1 f(r)[\eta u]_r z dr - \alpha_2 V_2 + \gamma \sup_{0\leq\tau\leq t}|\tilde{P}_{lh}(\tau)| \quad \text{(A.7)}$$

which in turn implies that:

$$\dot{V} \leq -\alpha V + \int_0^1 f(r)[\eta u]_r z dr + \gamma \sup_{0\leq\tau\leq t}|\tilde{P}_{lh}(\tau)| \quad \text{(A.8)}$$

where $\alpha \doteq \min\{\alpha_1, \alpha_2\}$. This completes the proof. □

Appendix B. Brief Introduction to Lyapunov Functions and Stability of Dynamical Systems

This section is intended to provide an intuitive overview of the use of Lyapunov functions for stability analysis of dynamical systems and is provided for pedagogical reasons only. For more precise results on Lyapunov theory for infinite dimensional systems, the reader can refer to [34] or [29]. For the use of strict Lyapunov functions in infinite dimensional systems, see [35].

Consider an autonomous (i.e. its evolution depending only on internal variables) finite-dimensional dynamical system with state vector $x(t) \in \mathbb{R}^n$ for all $t \in [0, T)$, whose evolution is given by:

$$\begin{aligned} \dot{x} \quad &= F(x), \forall t \in [0, T) \\ x(0) &= x_0 \end{aligned} \tag{B.1}$$

where $F : \mathbb{R}^n \to \mathbb{R}^n$ is a (possibly nonlinear) Lipschitz function and $\dot{x}$ denotes the time-derivative of x.

The origin of system (B.1) is defined as a *Globally Asymptotically Stable* equilibrium if for every initial state $x_0 \in \mathbb{R}^n$, $\|x(t)\| < +\infty$ for all $t \in [0, T)$ and $\|x(t)\| \to 0$ as $t \to +\infty$, where $\|\cdot\|$ is a norm in $\mathbb{R}^n$. It is a *Globally Exponentially Stable* equilibrium if for every initial state $x_0 \in \mathbb{R}^n$, $\|x(t)\| \leq ce^{-\alpha t}\|x_0\|$ for all $t \in [0, T)$, for some positive constants c, α.

A continuously differentiable candidate Lyapunov function $V(x)$ for the system (B.1) has to verify several technical conditions, in particular [36]:

- $V(0) = 0$;
- $V(x) > 0$ for all $x \neq 0$;
- $V(x) \to +\infty$ as $\|x\| \to +\infty$;
- $V(x)$ is bounded above and below by $\beta(\|x\|)$ and $\delta(\|x\|)$, respectively, two smooth increasing functions such that $\beta(0) = \delta(0) = 0$.

These conditions make a candidate Lyapunov function analogous to a potential or energy function in a physical system. If it can be shown that $\dot{V} \doteq \frac{\partial V}{\partial x} \cdot \dot{x} = \frac{\partial V}{\partial x} \cdot f(x) \leq 0$ for all $x \in \mathbb{R}^n$ with the equality occurring only for $x = 0$, then V is called a global Lyapunov function. The existence of a global Lyapunov function guarantees the global asymptotic stability of the origin of system (B.1).

If the Lyapunov function further satisfies, for some positive constant c, $\dot{V} \leq -cV(x)$ for all $x \in \mathbb{R}^n$, it is called a *strict* Lyapunov function [30]. The existence of a global strict Lyapunov function equivalent to the chosen norm in $\mathbb{R}^n$ guarantees the global exponential stability of the origin of system (B.1).

References

[1] A. Pironti and M. Walker. Fusion, tokamaks, and plasma control: an introduction and tutorial. *IEEE Control Systems Magazine*, 25(5):30–43, 2005.

[2] M.L. Walker, D.A. Humphreys, D. Mazon, D. Moreau, M. Okabayashi, T.H. Osborne, and E. Schuster. Emerging applications in tokamak plasma control. *IEEE Control Systems Magazine*, 26(2):35–63, 2006.

[3] T. S. Taylor. Physics of advanced tokamaks. *Plasma Phys. Control. Fusion*, 39:B47–73, 1997.

[4] C. Gormezano. High performance tokamak operation regimes. *Plasma Phys. Control. Fusion*, 41:B367–80, 1999.

[5] R. C. Wolf. Internal transport barriers in tokamak plasmas. *Plasma Phys. Control. Fusion*, 45:R1–91, 2003.

[6] E. Witrant, E. Joffrin, S. Brémond, G. Giruzzi, D. Mazon, O. Barana, and P. Moreau. A control-oriented model of the current control profile in tokamak plasma. *Plasma Phys. Control. Fusion*, 49:1075–1105, 2007.

[7] J. F. Artaud et al. The CRONOS suite of codes for integrated tokamak modelling. *Nucl. Fusion*, 50, 043001, 2010. http://dx.doi.org/10.1088/0029-5515/50/4/043001.

[8] T. Wijnands, D. Van Houtte, G. Martin, X. Litaudon, and P. Froissard. Feedback control of the current profile on Tore Supra. *Nucl. Fusion*, 37:777–791, 1997.

[9] O. Barana, D. Mazon, L. Laborde, and F. Turco. Feedback control of the lower hybrid power deposition profile on Tore Supra. *Plasma Phys. Control. Fusion*, 49:947–967, 2007. http://dx.doi.org/10.1088/0741-3335/49/7/001.

[10] F. Imbeaux, M. Lennholm, A. Ekedahl, P. Pastor, T. Aniel, S. Bremond, J. Decker, P. Devynck, R. Dumont, G. Giruzzi, P. Maget, D. Mazon, A. Merle, D. Molina, P. Moreau, F. Saint-Laurent, J.L. Segui, D. Zarzoso, and Tore Supra Team. Real-time control of the safety factor profile diagnosed by magneto-hydrodynamic activity on the Tore Supra tokamak. *Nuclear Fusion*, 51, 073033, 2011. http://dx.doi.org/10.1088/0029-5515/51/7/073033.

[11] L. Laborde et al. A model-based technique for integrated real-time profile control in the JET tokamak. *Plasma Phys. Control. Fusion*, 47:155–183, 2005.

[12] P. Moreau et al. Plasma control in Tore Supra. *Fusion Science and Technology*, 56:1284–1299, October 2009.

[13] D. Moreau et al. Plasma models for real-time control of advanced tokamak scenarios. *Nucl. Fusion*, 51(6), 2011. http://dx.doi.org/10.1088/0029-5515/51/6/063009.

[14] Y. Ou, C. Xu, E. Schuster, T. C. Luce, J. R. Ferron, M. L. Walker, and D. A. Humphreys. Optimal tracking control of current profile in tokamaks. *IEEE Transactions on Control Systems Technology*, 19(2):432–441, March 2011.

[15] A. Gahlawat, M. M. Peet, and E. Witrant. Control and verification of the safety-factor profile in tokamaks using sum-of-squares polynomials. In *Proceedings of the 18th IFAC World Congress. Milan, Italy*, volume 18, August, 2011. http://dx.doi.org/10.3182/20110828-6-IT-1002.02600.

[16] O. Gaye, E. Moulay, S. Brémond, L. Autrique, R. Nouailletas, and Y. Orlov. Sliding mode stabilization of the current profile in tokamak plasmas. In *Proceedings of the 50th IEEE Conference on Decision and Control and European Control Conference*, pages 2638–2643, 2011. http://dx.doi.org/10.1109/CDC.2011.6160442.

[17] F. Bribiesca Argomedo, C. Prieur, E. Witrant, and S. Brémond. Polytopic control of the magnetic flux profile in a tokamak plasma. In *Proceedings of the 18th IFAC World Congress. Milan, Italy*, volume 18, August, 2011. http://dx.doi.org/10.3182/20110828-6-IT-1002.01067.

[18] F. Bribiesca Argomedo, C. Prieur, E. Witrant, and S. Brémond. A strict control Lyapunov function for a diffusion equation with time-varying distributed coefficients. *To appear, IEEE Transactions on Automatic Control*, 2012. http://dx.doi.org/10.1109/TAC.2012.2209260.

[19] E. Zuazua. Approximate controllability for semilinear heat equations with globally lipschitz nonlinearities. *Control and Cybernetics*, 28(3):665–683, 1999.

[20] J.-M. Coron and E. Trélat. Global steady-state controllability of one-dimensional semilinear heat equations. *SIAM J. Control Optim.*, 43(2):549–569, 2004.

[21] M. Krstic and A.T. Smyshlyaev. Adaptive boundary control for unstable parabolic PDEs–part I: Lyapunov design. *IEEE Transactions on Automatic Control*, 53(7):1575–1591, 2008.

[22] A. Smyshlyaev and M. Krstic. Closed-form boundary state feedback for a class of 1-D partial integro-differential equations. *IEEE Transactions on Automatic Control*, 49(12):2185–2201, 2004.

[23] A. Smyshlyaev and M. Krstic. On control design for PDEs with space-dependent diffusivity or time-dependent reactivity. *Automatica*, 41:1601–1608, 2005.

[24] R. Vazquez and M. Krstic. *Control of Turbulent and Magnetohydrodynamic Channel Flows Boundary Stabilization and State Estimation*. Systems & Control: Foundations & Applications. Birkhäuser, 2008.

[25] F. Bribiesca Argomedo, E. Witrant, and C. Prieur. D1-input-to-state stability of a time-varying nonhomogeneous diffusive equation subject to boundary disturbances. In *Proceedings of the 2012 American Control Conference, Montréal, Canada*, pages 2978–2983, 2012.

[26] J. F. Artaud. *METIS user's guide*. CEA/IRFM/PHY/NTT-2008.001, 2008.

[27] J. Blum. *Numerical Simulation and Optimal Control in Plasma Physics*. Wiley/Gauthier-Villars Series in Modern Applied Mathematics. Gauthier-Villars, John Wiley & Sons, 1989.

[28] F. Kazarian-Vibert et al. Full steady-state operation in Tore Supra. *Plasma Phys. Control. Fusion*, 38:2113–2131, 1996.

[29] R. Curtain and H. Zwart. *An Introduction to Infinite-Dimensional Linear Systems Theory.*

Springer Verlag, 1995.

[30] E. D. Sontag. Input to state stability: Basic concepts and results. In *Nonlinear and Optimal Control Theory*, pages 163–220. Springer-Verlag, Berlin, 2007.

[31] J. Blum, C. Boulbe, and B. Faugeras. Reconstruction of the equilibrium of the plasma in a Tokamak and identification of the current density profile in real time. *Journal of Computational Physics*, 231(3):960–980, 2012.

[32] F. Felici, O. Sauter, S. Coda, B.P. Duval, T.P. Goodman, J-M. Moret, J.I. Paley, and the TCV Team. Real-time physics-model-based simulation of the current density profile in tokamak plasmas. *Nuclear Fusion*, 51, 2011. http://dx.doi.org/10.1088/0029-5515/51/8/083052.

[33] M. Goniche et al. Lower hybrid current drive efficiency on Tore Supra and JET. *16th Topical Conference on Radio Frequency Power in Plasmas. Park City, USA, April 2005.*

[34] Z.-H. Luo, B.-Z. Guo, and O. Morgul. *Stability and Stabilization of Infinite Dimensional Systems with Applications.* Communications and Control Engineering. Springer Verlag, 1999.

[35] F. Mazenc and C. Prieur. Strict Lyapunov functions for semilinear parabolic partial differential equations. *Mathematical Control and Related Fields*, 1(2):231–250, 2011.

[36] H. K. Khalil. *Nonlinear Systems.* Prentice-Hall, New Jersey, 1996.